LIGO Laboratory / LIGO Scientific Collaboration

LIGO-T030062-03-D 4/1/2003

Thermal Compensator Retrofit for LIGO I

M. Zucker, D. Ottaway, K. Mason

Distribution of this document:
Detector Revision Technical Review Board

This is an internal working note
of the LIGO Laboratory.

California Institute of Technology
LIGO Project – MS 18-34
1200 E. California Blvd.
Pasadena, CA 91125
Phone (626) 395-2129
Fax (626) 304-9834
E-mail: info@ligo.caltech.edu

Massachusetts Institute of Technology
LIGO Project – NW17-161
175 Albany St
Cambridge, MA 02139
Phone (617) 253-4824
Fax (617) 253-7014
E-mail: info@ligo.mit.edu

LIGO Hanford Observatory
P.O. Box 1970
Mail Stop S9-02
Richland WA 99352
Phone 509-372-8106
Fax 509-372-8137

LIGO Livingston Observatory
P.O. Box 940
Livingston, LA 70754
Phone 225-686-3100
Fax 225-686-7189

http://www.ligo.caltech.edu/

Introduction

The initial LIGO core optics design depends on thermal lensing in the arm cavity input couplers (ITM's) to stabilize the spatial mode of the recycling cavity[1]. The effect has minimal influence on the carrier, which is spatially stabilized by the long arm cavities, but strongly affects the coupling of the RF sensing sidebands, which resonate only in the recycling cavity. Preliminary measurements indicate as-built core optic absorption may be insufficient to form the necessary lens even at full operating power. This will also degrade performance more than necessary, should full design power prove elusive (e.g., due to laser aging) or should absorption increase in situ (e.g., due to contamination). A compromise in shot noise limited strain performance may result unless some means is introduced to match the lensing to as-built conditions.

Additionally, significant delays and operational inconveniences arise from starting the interferometer cold with a different optical character than its steady state, even if that condition is eventually optimized. Among these are the transient degradation of sensitivity (which adds to the downtime from each loss of lock) and a need to accommodate evolving alignment and length readout matrix elements between acquisition and steady state. In particular, the planned steady-state overcoupling of the sidebands leads to a sign reversal in common mode matrix elements, since the initial "cold" state is intrinsically undercoupled. This will present a "handoff" challenge to lock acquisition once design power is achieved.

We propose to retrofit a limited form of adaptive thermal lens control[2,3] into LIGO I. This system will act by externally modifying the thermal gradients in the core optics.

Anticipated requirements

The limited diagnostic results to date make formal requirements premature. A separate Design Requirements Document (DRD) will be issued for review as measurements are refined. However, internal discussions and prior work directed at problems in Advanced LIGO design have exposed what appear to be the most significant constraints. These appear sufficient to formulate the following conceptual design.

---

[1] W. Kells and J . Camp, *Absorption in the Core Optics and LIGO Sensitivity* . LIGO-T970097-01-D (1998).

[2] R. Lawrence, *Active Wavefront Correction in Laser Interferometric Gravitational Wave Detectors*. Ph.D. dissertation, Massachusetts Institute of Technology (2003).

[3] R. Lawrence, M. Zucker, P. Fritschel, P. Marfuta, and D. Shoemaker, "Adaptive thermal compensation of test masses in advanced LIGO," *Class. Quantum Grav.* 19 1803-1812 (2002); LIGO-P010023-00-R.

.

Noninvasive installation

There appears to be no solution that completely avoids breaking vacuum. Nevertheless, we should minimize the time each volume is at atmosphere, and the degree of human ingress during this time, to limit water vapor loading of Flourel parts and seals.

Similarly, we wish to avoid adding mass moments to isolation stack payloads or subjecting suspensions to installation forces and torques. This will limit risks of time-consuming realignment, or even damage, as well as the associated increased downtime at atmospheric pressure.

Dynamic Range of Corrections

We require our mechanism must to compensate for insufficient beam heating as well as excess heating, if possible, such that sideband coupling can be optimized in either condition. This constraint may be modified if further measurements argue otherwise.

Operationally, there is a powerful case for affording the capability to stabilize the sidebands in the recycling cavity even with *no* heat from absorption of the main beam. This will permit

- "cold start" with optimized sidebands and corresponding good sensitivity
- riding out dropouts with rapid recovery
- improved lock acquisition with better initial sensing matrix conditioning (maybe)
- diagnostics at low power, without sideband spatial mode degradation, and
- "soft" failure in the event of laser or input optics degradation.

This concern bounds the maximum "positive" lens we must provide, i.e., that amount assumed in the original core optics design for optimized sideband coupling (corresponding to about 25 mW deposited in each ITM). Additional margin is required to accommodate worst-case tolerances of the core optics and the compensation mechanism itself.

The maximum "negative" thermal lens is not so clearly bounded. Several tentative criteria have been proposed:

- afford capability to optimize at, e.g, twice the design power, in case a second power amplifier is added to the existing MOPA laser
- accomodate additional circulating field absorption (e.g., from accidental or cumulative contamination) perhaps up to a level comparable to scattering losses, without breaking vacuum to clean the optics
- simply bracket uncertainties (currently substantial) and accommodate differentials within an interferometer

We expect the achievable level of "negative" lensing to be much more constrained by engineering concerns, so we need to consider this requirement carefully.

Noise due to corrector fluctuations

We constrain any displacement noise added by the system to the usual 1/10 SRD equivalent displacement noise limits.

Displacement noise is expected through interaction of intensity noise in the heating mechanism with refractive index of the ITM, with thermal expansion of the cavity mirror surface, and with photon momentum recoil of the mirror (Appendix B).

Collateral heating

Stray heating of unintended components must not risk damage or cause misalignment through thermal expansion.

Proposed Approach

Because of the limited development schedule and resources, we initially looked at a simple shielded heating ring as described by Lawrence. This approach has (at least) two critical disadvantages. First, such a heater and shield would need to be attached to LOS or SEI structures, requiring extended periods at atmosphere with people inside[4] and risking misalignment or damage. Second, while calculations show that a "positive lens" can in principle be generated by suitable arrangement of shields and radiators without violating the beam aperture, such a design has never been tested. Even if a satisfactory design is developed on paper, there currently exists no suitable off-line experimental testbed; any design iteration would therefore multiply the downtime and vacuum incursion concerns discussed above.

Directed Beam Actuator

As a result we looked more seriously at the other mechanism described by Lawrence, directed-beam heating. Preliminary survey of the system-level optical layouts for the three interferometers indicate possible direct paths to illuminate all six LIGO ITM's from existing viewport flange locations. If such paths prove tractable, the installation might be no more invasive (from the vacuum standpoint) than substitution of a compatible viewport in each location. Because of the small surface area of the breach, this port change can be performed while maintaining outward laminar flow of dry backfill air, thereby introducing little or no water vapor.

For the 4km L1 and H1 interferometers the proposed paths shoot from ports below beamline level on the [-X] and [-Y] sides of the beamsplitter chamber, WBSC2 and LBSC2, toward the back (AR) face of the respective ITM's (Figure 1).

[4] Time to desorb water vapor to a level precluding beam tube contamination is a sharp function of time at atmosphere and degree of exposure. Several days open with workers inside may translate into months of downtime for degassing before the beam tube isolation valves can be safely reopened.

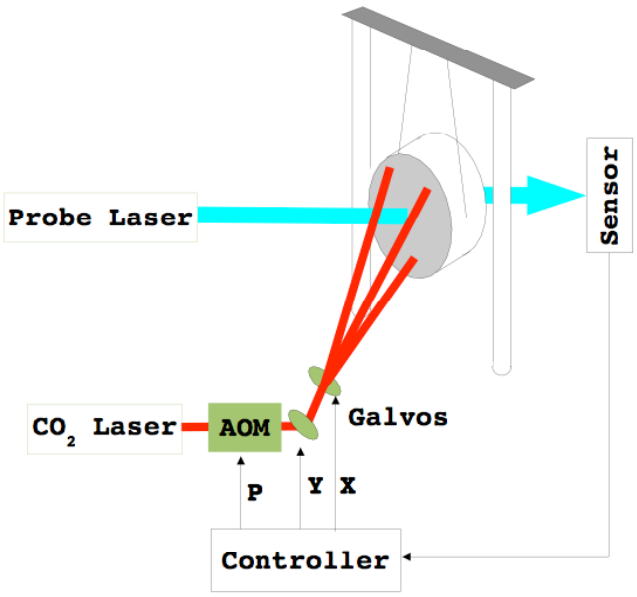

Figure 1. Scanned directed beam thermal compensator concept.

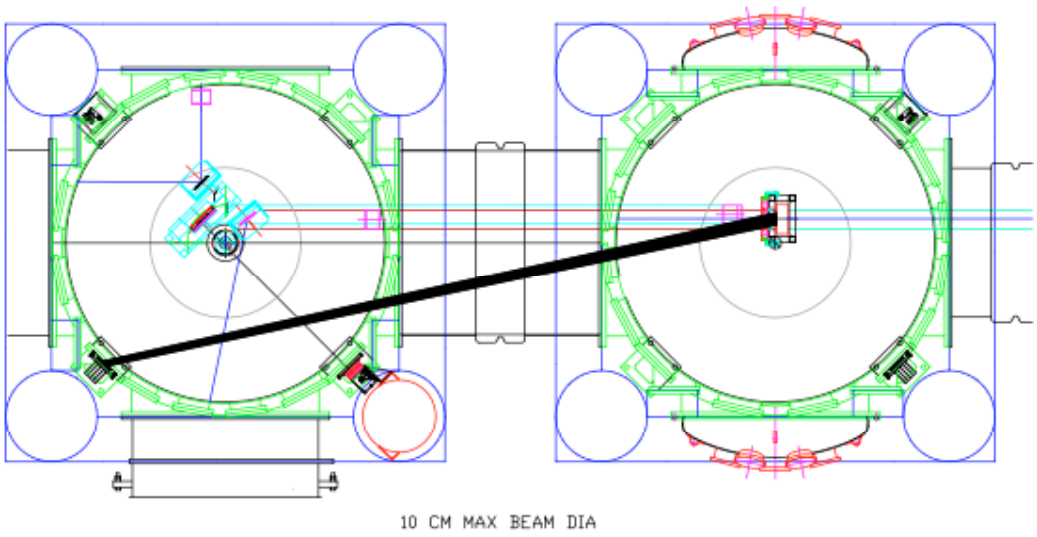

Figure 2. Possible compensator beam layout for H1 and L1 (ITMx shown). The ITM elliptical baffle limits the maximum centered aperture on the ITM AR face to approximately 10 cm diameter.

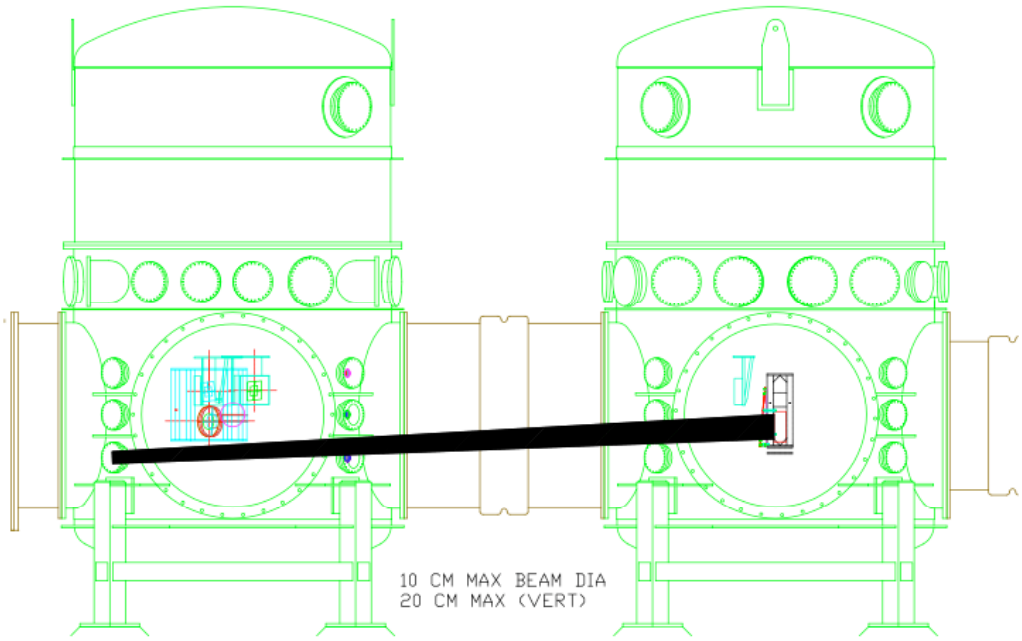

Figure 3. Elevation view of 4k thermal actuator beam path.

For the 2km H2, one path appears to be approximately parallel with the face of each fold mirror, using similar ports on the diagonals of the respective ITM chambers themselves (WBSC7 and WBSC8). The angle of incidence for this latter view is over 40 degrees with respect to the ITM face normal; the compensator would therefore need to accommodate the resulting astigmatism. More seriously, the elliptical glass baffles (not shown in the ILD) severely restrict the aperture available off normal incidence, such that even a cavity-waist size compensation beam would not fit.

Three alternative options are under discussion. One is to violate the constraint against incursions into the vacuum chamber, to insert a lightweight IR steering mirror (e.g., copper or evaporated gold on aluminum). This path is illustrated in Figure 4.

Another interesting option is to forego actuating the ITM at all and heat the faces of the fold mirrors (Figure 5). Although the effect in this case would be entirely due to thermal expansion of the fold mirror surface, which is comparatively ineffective, the insensitivity of the fold mirror to phase noise might permit correspondingly higher compensator power without excess noise generation.

Finally, it may be feasible to actuate directly on the cavity mirror HR surface (Figure 6). Although thermal expansion of the cavity mirror increases the sensitivity to

compensating laser intensity fluctuations by about a factor of five (Appendix B), the requisite enhanced intensity stabilization may be achievable.

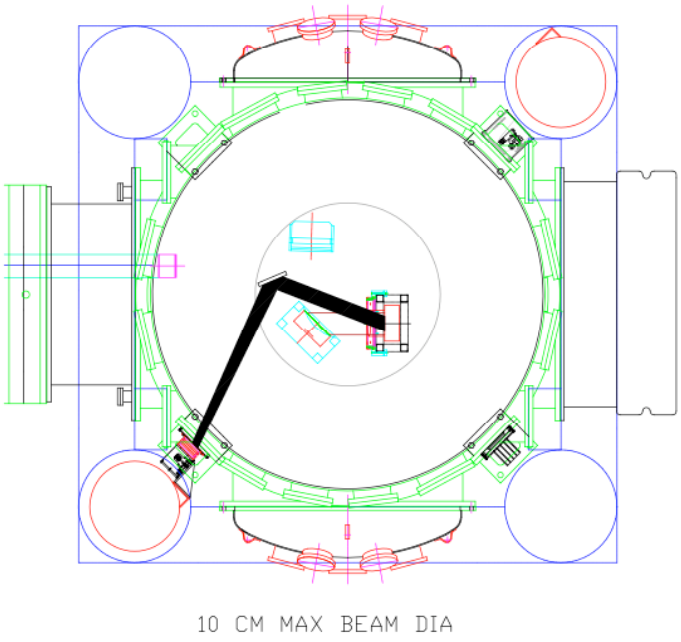

Figure 4 Possible beam path for H2 ITMx using additional in-vacuum redirection mirror. Mirror is approximately 20 cm above interferometer plane to avoid interference with H1 beam path. The elliptical baffle limits the maximum centered aperture on the ITM surface to approximately 10 cm diameter.

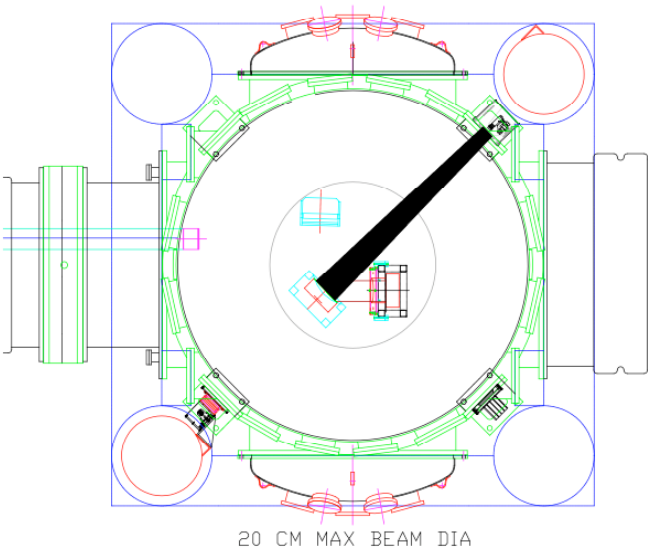

Figure 5. Alternate H2 beam path with actuation on face of fold mirror.

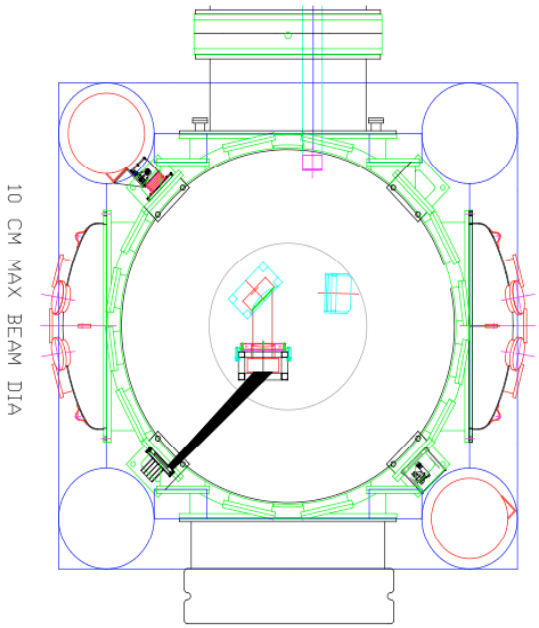

Figure 6. Alternate H2 (or H1) beam path involving actuation on front HR surface of ITM.

Staring beam actuator

The scanned-beam approach also has difficulties. One is that the galvanometer beam steering system is expensive and may require substantial software investment. A more serious worry is the possibility of introducing noise into the ITM's through the time-dependent scanning and modulation of the heating beam. In Advanced LIGO, we plan to actuate on separate transparent compensator plates that do not influence the cavity length to lowest order; in this system, we are bound to actuate directly on the ITM's.

One of us (DO) proposed resurrecting an older idea, namely a staring actuator which projects a CW intensity pattern onto the optic. The approach was previously abandoned for technical reasons; an arbitrary-pattern electrooptic spatial light modulator (SLM) could not be found for heating beam wavelengths, like 10.6 μm (CO_2). However, under the reasonable present assumption that here the required lensing is axisymmetric and simple in form, a fixed pattern mask could be used instead. Such masks could be physically interchanged to accommodate gross evolution (e.g., from positive to negative lensing). However, simple imaging and power adjustments permit "active" optimization of the depth and transverse spatial scale of the heat pattern, as well as its centering. In principle, slightly more complicated imaging arrangements could also provide active adjustments for the degree and principal axis of ellipticity.

The general scheme is presented conceptually in Figure 8. Clearly there are numerous detailed design issues to resolve (see below). However, assuming we can successfully introduce the compensator beam with no in-vacuo components, any required iteration of the design can proceed with little or no interference with other commissioning activities, and particularly with no further vacuum envelope incursions after the viewport installation.

System components description

Laser

The least expensive laser suitable for heat deposition in fused silica appears to be the common CO_2 laser operating at 10.6 μm wavelength[5]. Depending on the efficiency of the imaging and the ultimate requirements (particularly for negative lensing) a modest 25 W system is expected to be adequate. Commercial sealed-tube systems are available with high beam quality ($M^2 < 1.2$) at modest cost ($3k to $6k depending on options). Longevity in service may be an issue, although several manufacturers guarantee over 15,000 hours, and tube refurbishment is economical and fast. Long-term intensity stability of a few % is typical; however, intensity and mode shape noise at audio frequencies are not known, and would have to be characterized. Similarly, RF interference is a concern, particularly for RF-excited tubes but also for DC systems, (which use switch-mode power supplies to achieve high voltage). It is likely that RFI containment will be an additional criterion placed on the required laser safety enclosure.

[5] We are looking in parallel at 1.5 and 3.5 μm solid-state laser systems, which might offer advantages in noise and power stability.

At the 25 W power level direct fan cooling and water cooling are both viable options; efficient CO_2 lasers dissipate only 10 to 20 watts per watt of useful output. Water cooling, while more complicated, is favored because it permits remote location of fans and AC-powered equipment well away from the test mass chambers (perhaps even outside the LVEA).

Acoustooptic intensity modulator

Precise DC control and broadband intensity stabilization, for reduction of intrinsic RIN, will likely require addition of an acoustooptic modulator. Commercial AO modulators for 10 μm wavelength are available in the range of $5k (TBR). Most designs require water cooling for operation at full RF (and optical) power. This may not be necessary if the AO adjustment dynamic range can be restricted to a small fraction of the mean power, with some other adjustment means (e.g., direct modification of the laser current) for gross variations.

Power monitor detector

The error sensor for intensity stabilization must be DC-coupled and preferably should not require cryogenic cooling. Photon-drag effect HgTeCd detectors marketed by Boston Electronics group are available in the $1k range; we have one in the MIT lab and will test it for stability. It is not clear if a separate monitoring detector will be needed in addition to the loop error sensor.

We expect a copy or minor variant of the existing PSL ISS (Intensity Stabilization Servo) electronics will serve for implementing the feedback loop for intensity stabilization.

Reflective intensity mask

For the case of increased central heating, as to compensate for lower-than-expected Nd:YAG power or absorption, it should be adequate to project a properly-sized and attenuated TEM_{00} beam onto the center of the optic. In this case the reflective mask will be a simple reflective attenuator, for example, evaporated gold on Ge or ZnS substrate. One complication is the test mass incidence angle afforded by available viewport locations, which would render the thermal pattern of an initially circular beam highly elliptical. In these cases, an elliptical mask may be used to avoid costly and complex astigmatic optics; we do not expect the loss of power efficiency to be an issue given the small anticipated heating loads.

For more complex compensation cases, for example the case of central overheating due to contamination, we expect that a "doughnut" shaped or more detailed mask can be prepared. We have not examined this in detail; in particular, we need to establish the constraints imposed by peripheral aperture obstructions.

The mask's spatial scale will be about the natural output beam diameter of the laser, typically 3 to 6 mm. We expect that if the mask is close to the laser it will not be strictly necessary to form a waist at the mask location.

Lateral alignment and diameter of the delivered pattern will be adjustable using motorized focus and steering mirror drives. Gross changes will have to be effected by exchanging aperture masks, which will be kinematically positioned to minimize need for realignment.

Visible guide laser

Aiming the heating beam will be tricky, since there is no convenient means to image this wavelength from outside, even if a (second) clear view can be negotiated. As an aid to initial and periodic alignment we add a collinear visible diode pilot laser beam to the CO_2 beam. This argues for making the imaging and viewport optics partially transmissive in the visible (e.g., ZnSe or ClearTran) and/or reflective. Since the central spot will be invisible on the superpolished ITM surface, we propose a crossed- line or bullseye alignment pattern generator (e.g., Lasiris Inc. LPG series) for this alignment beam. The co-collimation of IR and visible guide beams is accomplished in the laboratory before installation.

Imaging optics

We will need to relay an image of the aperture mask onto the ITM surface. This can be accomplished using a single lens whose reciprocal focal length is the sum of the reciprocals of mask-lens and lens-ITM distances. In practice we will synthesize this "lens" from a convex/concave pair of mirrors whose separation and axial position are adjustable to admit independent tuning of focal length and object distance. Commercial off-axis paraboloid IR beam expanders and ZnSe lens systems are under consideration for this assembly. Focal performance at the visible guide laser wavelength will be considered in making this choice.

IR viewports become expensive and potentially fragile in nominal apertures greater than 50 mm. Because beam entry will typically be off normal incidence, we wish to constrain the beam diameter at the viewport to a maximum diameter of about 36 mm. We expect this will be feasible since all possible entry ports are at least 2m from the relevant ITM face.

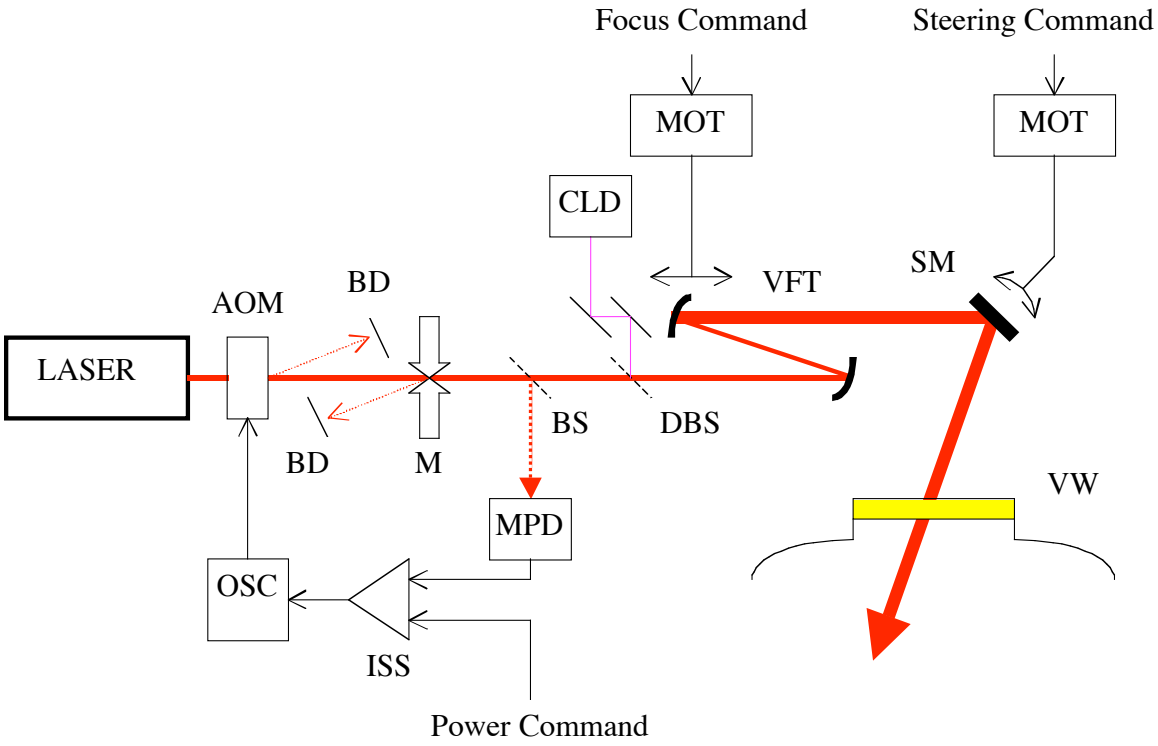

Figure 8. Staring-beam thermal compensator concept. KEY: AOM; acoustooptic intensity modulator, OSC; variable-output RF drive oscillator, BD; beam dump, M; reflective intensity mask, CLD; collimated laser diode pilot laser, BS; beamsplitter, DBS; dichroic beamsplitter, MPD; monitoring photodetector, ISS; intensity stabilization servocontroller, VFT; variable-focus beam expander, MOT; mirror motion control driver, SM; steerable mirror, VW; IR + visible transmitting vacuum window.

Some open design issues

Formation of usable "negative" lens given aperture restriction

The horizontal restriction imposed by the elliptical scatter baffles, combined with the off-axis illumination direction, limits the maximum circular intensity field that can be centered on the AR surface of the ITM. Current layouts suggest this limit is no more than 10 cm diameter, only about 3 Gaussian beam radii. It is not clear to what degree a feasible distribution of corrective heat within this zone can adequately counteract excess absorption from the main beam.

Intensity stabilization of CO_2 laser

As shown in the Appendix, avoiding excess noise requires intensity stability better than 2×10^{-5} $Hz^{-1/2}$ near 150 Hz. Comparable performance is readily achieved in stabilized gas and solid state lasers, but we are not currently aware of prior applications requiring or demonstrating stabilization at this level for a CO_2 laser system. Laser spatial mode

instability and spatial nonuniformity of mid-IR photodetectors could introduce sensing errors for such a stabilization system, and will need characterization.

Heat required to effect correction on fold mirrors

The practical convenience of actuating on the fold mirrors in the H2 instance carries a cost in significantly higher required power for a given correction. An exact calculation must take account of the constrained thermoelastic deformation, but for a "convex" correction the increase will be roughly the ratio of index temperature coefficient β to thermal expansion coefficient α, about 18:1. This suggests power delivery in the 0.5 W range (compared to 25 mW for index actuation). Since the smallest available CO_2 laser system puts out 10W this should not be an issue, but we need to verify that safety and collateral heating concerns (below) are not complicated. A more serious concern is whether any amount of heat can produce a "concave" correction, given that the overall expansion of the heated face invariably produces a net convex bowing of the optic.

Collateral heating

The Fresnel reflections from test mass surfaces could be deliberately blocked to avoid inadvertent heating of other components. However placement of beam dumps would require ingress into the vacuum envelope. Since the incident power required is relatively low (25 mW) and the beam will be fairly diffuse, there should be no problem simply letting ghost beams fall where they will. Note that normal glass and silica viewports are opaque at 10.6 μm wavelength, so there is no safety issue.

If we choose to actuate by thermal expansion on the fold mirrors higher power will be introduced. In this case, however, the beam path is fairly simple and unobstructed (Figure 5) so return power should dump harmlessly on the BSC wall.

Safety

The addition of Class IV lasers to the LVEA will require adjustment of the laser SOP's, but the adjustment is minor. Essentially all existing eyewear will simultaneously block 10.6 μm radiation at the required OD. As with all LIGO laser equipment, installations will be CDRH compliant, e.g., requiring full enclosures openable only with tools, and redundant protection features.

Appendix A: Required Heat to Stabilize Recycling Cavity

The original design[6] calls for approximately 25 mW of heat to be deposited in each ITM by the resonating 1.064 μm beam, divided about equally between surface heating (0.6 ppm coating absorption from 18 kW cavity circulating power) and bulk substrate absorption (0.5 ppm/cm bulk absorption over 10 cm mirror thickness with 150 W circulating in 2 passes). Although compensation of a negative lens (due to excess beam heating) would probably be inefficient, requiring more compensation power, the pattern

[6] W. Kells and J. Camp, *Absorption in the Core Optics and LIGO Sensitivity*. LIGO-T970097-01-D (1998).

would avoid the center, so the following noise effects (other than radiation pressure) would be mitigated. As a result we baseline our results for 25 mW applied in the heating beam.

Appendix B: Effects of RIN in a Heating Laser

Here we calculate the maximum allowable relative intensity noise (RIN) on a heating laser beam. Our criterion is to bound any resulting mirror displacement at 1/10 the LIGO Science Requirement differential arm length amplitude spectral density[7] The relevant benchmark frequencies are 40 Hz and 150 Hz, where "SRD/10" demands displacement spectral densities

$$\tilde{x}(40\ \mathrm{Hz}) < 1.0 \cdot 10^{-19}\ \frac{\mathrm{m}}{\sqrt{\mathrm{Hz}}}$$

and

$$\tilde{x}(150\ \mathrm{Hz}) < 1.0 \cdot 10^{-20}\ \frac{\mathrm{m}}{\sqrt{\mathrm{Hz}}}.$$

To summarize, we find the limiting mechanism to be local index fluctuation in the ITM substrate due to relative intensity noise in the compensating laser. The above criterion limits this relative intensity noise to $\mathrm{RIN}(150\ \mathrm{Hz}) < 2 \cdot 10^{-5}\ \mathrm{Hz}^{-1/2}$ for 25 mW correction power. If the correction is applied to the HR face of the mirror instead of the AR surface, the additional contribution of surface thermal expansion requires a further reduction in allowable RIN, by about a factor of 5.

Photon momentum recoil

Under the assumption that the heating laser power P_A is fully absorbed at normal incidence from only one side of each ITM, the resulting displacement spectral density due to momentum transfer from the beam is

$$\tilde{x}_{\mathrm{rp}}(f) = \sqrt{N} \cdot \left| \frac{\tilde{P}_A(f)}{\langle P_A \rangle} \right| \cdot \frac{\langle P_A \rangle}{(2\pi f)^2 M c}$$

$$\approx 10^{-19}\ \frac{\mathrm{m}}{\sqrt{\mathrm{Hz}}} \cdot \left(\frac{40\ \mathrm{Hz}}{f} \right)^2 \cdot \left(\frac{\langle P_A \rangle}{25\ \mathrm{mW}} \right) \cdot \left[\frac{\mathrm{RIN}}{5.4 \cdot 10^{-4}\ \mathrm{Hz}^{-1/2}} \right]$$

where f is the frequency, M is the mass (10 kg), N is the number of mirrors actuated (2, with the assumption that their fluctuations are uncorrelated), and

$$\mathrm{RIN} \equiv \left| \frac{\tilde{P}_A(f)}{\langle P_A \rangle} \right|$$

[7] A. Lazzarini and R. Weiss, *LIGO Science Requirements*. LIGO-E950018-02-E (1996).

is the "relative intensity noise" (amplitude spectral density of fractional power fluctuations). We evaluate this noise mechanism at 40 Hz, since it falls as f^{-2} in parallel with the SRD curve for constant RIN.

Thermal expansion and index change of entire test mass

For illustration we consider a limiting case in which the thermal conductivity of the test mass is presumed very high, such that internal thermal equilibrium is obtained at all relevant timescales. In this limit the uniform body temperature is determined by balance between deposited energy, stored heat and radiation from the surface. Approximating both test mass and ambient environment as black bodies (emissivity $\epsilon = 1$), we find

$$\frac{\delta T_R}{\langle P_A \rangle} = \frac{1}{4\sigma A T_0^3} \approx 0.92 \frac{^\circ\mathrm{K}}{\mathrm{W}}$$

where A is the area of the test mass (about 0.18 m^2), T_0 is the ambient temperature (300°K) and σ is the Stefan- Boltzmann constant. The radiative equilibration time constant is given by

$$\tau_R = \frac{MC}{4\sigma A T_0^3} = MC \cdot \frac{\delta T_R}{\langle P_A \rangle} \approx 6{,}854 \text{ s} \sim 2 \text{ h}$$

where C is the specific heat (745 J kg^{-1} °K^{-1}).

The optical effect due to varying power comprises two effects; thermal expansion of the test mass, which displaces the reflective face with respect to the center of mass, and alteration of the refractive index of the substrate, which alters the optical phase on transmission. The latter effect is diminished by a factor of the cavity power buildup, such that the total effect is given by

$$\tilde{x}_R(f) \approx \sqrt{N} \cdot \mathrm{RIN} \cdot \frac{\delta T_R}{2\pi f \tau_R} \cdot \frac{h}{2} \left(\alpha + \frac{\beta}{\mathcal{F}} \right)$$

$$\approx 10^{-20} \frac{\mathrm{m}}{\sqrt{\mathrm{Hz}}} \cdot \left(\frac{150 \text{ Hz}}{f} \right) \cdot \left(\frac{\langle P_A \rangle}{25 \text{ mW}} \right) \cdot \left(\frac{\mathrm{RIN}}{6 \cdot 10^{-5} \text{ Hz}^{-1/2}} \right)$$

where h is the test mass thickness (10 cm), α is the thermal expansion coefficient (5.5x10^{-7} °K^{-1}), $\beta \equiv \frac{dn}{dT}$ is the temperature coefficient of refractive index (10^{-5} °K^{-1}) and $\mathcal{F}$ is the arm cavity finesse (about 200). This effect is evaluated at 150 Hz since it falls more slowly than the SRD requirement spectrum with increasing frequency.

The approximation of high conductivity is grossly optimistic, of course. However, it's worth noting that the radiative time constant τ_R found above is large enough that we can safely neglect radiative boundary conditions in noise calculations; for relevant fluctuation timescales, the mirror may be treated as an infinite half-space.

Internal thermal gradient, heat applied to HR face

A more realistic heat flow model considers radial conduction of heat away from a deposition zone of size determined by the heating beam radius *w*. Following Winkler et al.[8] the central temperature rise with respect to the edge per unit power deposited by a Gaussian beam of $1/e^2$ radius w = 3.6 cm is approximately

$$\frac{\Delta T_w}{\langle P_A \rangle} = \frac{1}{2\pi\kappa w} \approx 3.2 \frac{^\circ\mathrm{K}}{\mathrm{W}}$$

where κ is the thermal conductivity (1.4 W m^{-1} °K^{-1}). The corresponding thermal time constant of the half-spherical subvolume of radius *w* is approximately

$$\tau_w = \frac{\rho w^2 C}{3\kappa} = \frac{\rho w^3 C}{6\kappa} \frac{\Delta T_w}{\langle P_A \rangle} \approx 506 \text{ s} \sim 8 \text{ m}$$

where ρ is the density (2200 kg m^{-3}).

The affected thermal zone penetrates about a beam radius deep. Following Braginsky et al.[9], the localized surface displacement component must include a factor of (1+σ), where σ is the Poisson ratio (σ~0.17). This accounts for local "buckling" of the surface, which is radially constrained by unheated material. Adding surface and index components, with the latter again derated by the cavity buildup, the total estimated optical effect is

$$\tilde{x}_w^{HR}(f) \approx \sqrt{N} \cdot \mathrm{RIN} \cdot \frac{\Delta T_w}{2\pi f \tau_w} \cdot \frac{w}{2} \left[\alpha (1+\sigma) + \frac{\beta}{F} \right]$$

$$\approx 10^{-20} \frac{\mathrm{m}}{\sqrt{\mathrm{Hz}}} \cdot \left[\frac{150 \text{ Hz}}{f} \right] \cdot \left[\frac{\langle P_A \rangle}{25 \text{ mW}} \right] \cdot \left[\frac{\mathrm{RIN}}{4 \cdot 10^{-6} \text{ Hz}^{-1/2}} \right] .$$

Internal thermal gradient, heat applied to AR face

Since most of the above effect is due to direct expansion of the cavity mirror surface, heating the back (AR) surface is safer if access is feasible (the desired effect on the recycling cavity stability will be about the same either way.)

In this case we can neglect the expansion term proportional to κ in the above expression and only keep the β (refractive index) term. This relaxes the required RIN by a factor of 4.7, such that

[8] *Phys. Rev. A* **44** (11), p. 7022 (1991)

[9] V.B. Braginsky, M. L. Gorodetsky, and S.P. Vyatchanin, *Phys. Lett. A*. 264 1 (1999).

$$\tilde{x}_w^{AR}(f) \approx \sqrt{N} \cdot \mathrm{RIN} \cdot \frac{T_w}{2\pi f_w} \cdot \frac{w}{2} \left| \frac{\partial}{\partial F} \right|$$

$$\approx 10^{-20} \frac{\mathrm{m}}{\sqrt{\mathrm{Hz}}} \cdot \left(\frac{150\ \mathrm{Hz}}{f} \right) \cdot \left(\frac{\langle P_A \rangle}{25\ \mathrm{mW}} \right) \cdot \left(\frac{\mathrm{RIN}}{2 \cdot 10^{-5}\ \mathrm{Hz}^{-1/2}} \right) .$$

Appendix C: Bowing of the opposite face

Addition of heat to the back face of the ITM (whether patterned to increase or decrease the radial temperature gradient) will cause collective thermoelastic expansion of that surface. This will "bow" the mirror, altering the HR face radius of curvature. This effect was analytically treated by Hello and Vinet[10], and this analysis corrected and verified numerically by Lawrence[11]. For the LIGO I fused silica optics, the resulting change in sagitta over the beam diameter is approximately 2 nm per watt of power absorbed on the opposite face.

We will use approximately .025 W, so the expected sagitta change is 0.5 Å or 0.1% of the nominal sag (55 nm). As shown in [12], this produces negligible changes in coupling into the arm cavities or contrast defect (if asymmetrical).

This effect always makes the heated face convex and the opposite face concave with applied heat.

[10] P. Hello and J.-Y.Vinet, "Analytical models of thermal aberrations in massive mirrors heated by high power laser beams." *J. Phys. France*, 51:1267-1282 (1990).

[11] R. C. Lawrence, *Active Wavefront Correction in Laser Interferometric Gravitational Wave Detectors*. Ph.D. dissertation, Massachusetts Institute of Technology (2003).

[12] Kells and Camp, op. cit.